

Hermano José Ribeiro Henriques<sup>(1)</sup> (✉), Dário Alexandre Schwambach<sup>(1)</sup>, Vanessa Jordão Marcato Fernandes<sup>(1)</sup> and Jorge Wilson Cortez<sup>(1)</sup>

<sup>(1)</sup>Universidade Federal da Grande Dourados - UFGD - Faculdade de Ciências Agrárias - FCA

E-mail: [hermano.henriques.hh@gmail.com](mailto:hermano.henriques.hh@gmail.com),  
[dario\\_schwambach@yahoo.com](mailto:dario_schwambach@yahoo.com),  
[vanessafernandes@ufgd.edu.br](mailto:vanessafernandes@ufgd.edu.br),  
[jorgecortez@ufgd.edu.br](mailto:jorgecortez@ufgd.edu.br).

✉ Corresponding author

## How to cite

HENRIQUES, H. J. R.; SCHWAMBACH, D. A.; FERNANDES, V. J. M.; CORTEZ, J. W. Vegetation indices and their correlation with second-crop corn grain yield in Mato Grosso do Sul, Brazil. *Revista Brasileira de Milho e Sorgo*, v. 20, e1195, 2021.

## VEGETATION INDICES AND THEIR CORRELATION WITH SECOND-CROP CORN GRAIN YIELD IN MATO GROSSO DO SUL, BRAZIL

**Abstract** – The emergence of satellites covering new electromagnetic wavelengths allowed developing different vegetation indices, enabling the study of their correlation with grain yield. In this sense, this study aimed to evaluate the accuracy between the mean values of seven vegetation indices and the mean corn grain yield in the field by applying linear regression equations. The indices NDVI, NDRE, GNDVI, GRNDVI, and PNDVI were used, with changes proposed in the equations of the indices GRNDVI and PNDVI, in which the red wavelength was replaced by the red edge. The multispectral bands provided by the Sentinel-2A and Sentinel-2B imaging instruments were used as a source of data to calculate the vegetation indices, while the values recorded by the grain harvester were used for the survey of grain yield data. A high correlation was observed between indices and grain yield. The replacement of the red wavelength with the red edge improves the correlation between vegetation indices and grain yield. Moreover, the indices GNDVI and NDVI easily saturate, reaching maximum values and not allowing the distinction between sample classes. Therefore, the vegetation indices PRENDVI and GRENDVI are recommended for estimating grain yield.

**Keywords:** Precision agriculture, orbital images, wavelengths.

## ÍNDICES DE VEGETAÇÃO E SUA CORRELAÇÃO COM A PRODUTIVIDADE DE GRÃOS DE MILHO EM SEGUNDA SAFRA NO MATO GROSSO DO SUL

**Resumo** - O surgimento de satélites abrangendo novos comprimentos eletromagnéticos de onda permitiu o desenvolvimento de diferentes índices de vegetação, possibilitando o estudo da correlação destes com a produtividade de grãos. Assim, este estudo teve como objetivo avaliar a acurácia entre valores médios de sete índices de vegetação e as produtividades médias de grãos da cultura do milho em campo, aplicando equações de regressão linear. Os índices utilizados foram: NDVI, NDRE, GNDVI, GRNDVI, e PNDVI, sendo propostas alterações nas fórmulas dos índices GRNDVI e PNDVI, substituindo o comprimento de onda do vermelho pelo do vermelho da borda (Red Edge). Como fonte de dados para o cálculo dos índices de vegetação foram utilizadas as bandas multiespectrais fornecidas pelos instrumentos imageadores Sentinel-2A e Sentinel-2B, e para o levantamento de dados de produtividade de grãos, valores registrados pela colhedora de grãos. Observou-se alta correlação entre os índices estudados e a produtividade de grãos. Verificou-se que a substituição do comprimento de onda vermelho pelo vermelho da borda melhora a correlação entre índices de vegetação e a produtividade de grãos, e que os índices GNDVI e NDVI saturam facilmente, atingindo valores máximos, não permitindo a distinção entre classes amostrais. Assim, os índices de vegetação recomendados para a estimativa da produtividade de grãos são o PRENDVI e o GRENDVI.

**Palavras-chave:** Agricultura de precisão, imagens orbitais, comprimentos de onda.

In recent decades, corn has reached the level of the most produced crop in the world, exceeding the 1 billion ton mark, which has left behind competing crops such as wheat and rice. The crop is still established in the world context as a parameter of food security (Contini et al., 2019).

The survey of the corn production potential is essential for each growing season. This process is influenced by the spatial variability in the field, requiring the adjustment of tools that assist in the decision-making. In this sense, remote sensing (RS) can be used as an auxiliary tool in monitoring plant health.

One of the most efficient and economical ways for terrestrial observation is associated with the satellite constellation, allowing the collection of data for the management of large areas. Researchers around the world have been looking to improve low-resolution image processing techniques, as they are available free of charge and provide extensive coverage and high temporal resolution. It allows detecting parameters related to plant development through the spatial and temporal survey of photosynthetic activity in the form of vegetation indices (VIs) through the reflection of electromagnetic radiation (EMR) from the crop canopy under analysis (Bertolin et al., 2017). For this, the most suitable period for the acquisition of images must coincide with the phenological stage of maximum crop development. This period is represented by the full tasseling in the corn crop, that is, the photosynthetic peak of the crop and a

determining factor for the best time to calculate VIs (Bertolin et al., 2017).

Vegetation indices are normalized mathematical equations based on EMR and its wavelengths: blue, green, red, and near-infrared (Bertolin et al., 2017). Ngie and Ahamed (2018) stated that the estimation of the photosynthetic activity of corn can be estimated using VIs and medium-resolution orbital images.

Red edge is a new alternative for estimating photosynthetic activity through VIs. Its wavelength extends between 680–740 nanometers, being allocated between the red and near-infrared electromagnetic spectra (Cui & Rekes, 2018). Kanke et al. (2016) stated that the red and red edge wavelengths are strongly absorbed by the chlorophyll pigments, while the near-infrared is reflected based on the leaf structure.

Geostatistics has been the best option in precision agriculture (PA) for the analysis of the spatial variation of yield from point data obtained in the field (Molin et al., 2015). One of the most popular interpolators is the inverse distance weighted (IDW) (Yamamoto & Landim, 2013).

Thus, this study aimed to evaluate the accuracy of seven vegetation indices for estimating the mean second-crop corn grain yield in the field.

## Material and methods

The study was carried out using orbital images from a commercial area of 19.25 ha

cultivated with the single hybrid corn Formula Viptera (Syngenta) under rainfed conditions in the second crop and located in Ponta Porã, State of Mato Grosso do Sul, Brazil, at coordinates 22°22'10.17" S and 55°11'5.04" W.

The soil is classified as a clay-textured dystrophic Red Latosol (Santos et al., 2018), with a flat relief and a mean altitude of 435 m.

The regional climate is Cwa according to the classification of Köppen & Geiger (1936), characterized as a humid temperate climate with a dry winter and hot summer.

The monthly mean data on precipitation and air temperature between January and August 2018, the year of this study, are shown in Figure 1.

Corn was sown on February 28, 2018, under a crop succession system, with a final population of 52,000 plants per hectare. Sowing fertilization was carried out in the furrow according to the

nutritional requirements of the corn crop by applying 165 kg ha<sup>-1</sup> of the formulation 08–20–20. Soil chemical and physical characteristics were obtained through laboratory analysis in the Department of Soil Fertility of the Federal University of Grande Dourados and consisted of a pH of 5.5, phosphorus of 13.8 mg dm<sup>-3</sup>, organic matter of 35.2 mg dm<sup>-3</sup>, potassium of 34.8 mg dm<sup>-3</sup>, calcium of 5.7 mg dm<sup>-3</sup>, magnesium of 1.2 mg dm<sup>-3</sup>, aluminum of 0.0 mg dm<sup>-3</sup>, sand of 34.2%, clay of 46.6%, and silt of 19.2%.

Orbital images of the Sentinel-2A and Sentinel-2B imaging instruments were acquired from April 24, 2018, when the corn crop was at the phenological stage VT (full tasseling) (Rosa et al. 2017). The images were downloaded through the United States Geological Survey (USGS) website, through the EarthExplorer (2018) page. The orbital images shown in Table 1 have a spatial resolution of 10 m for the wavelengths

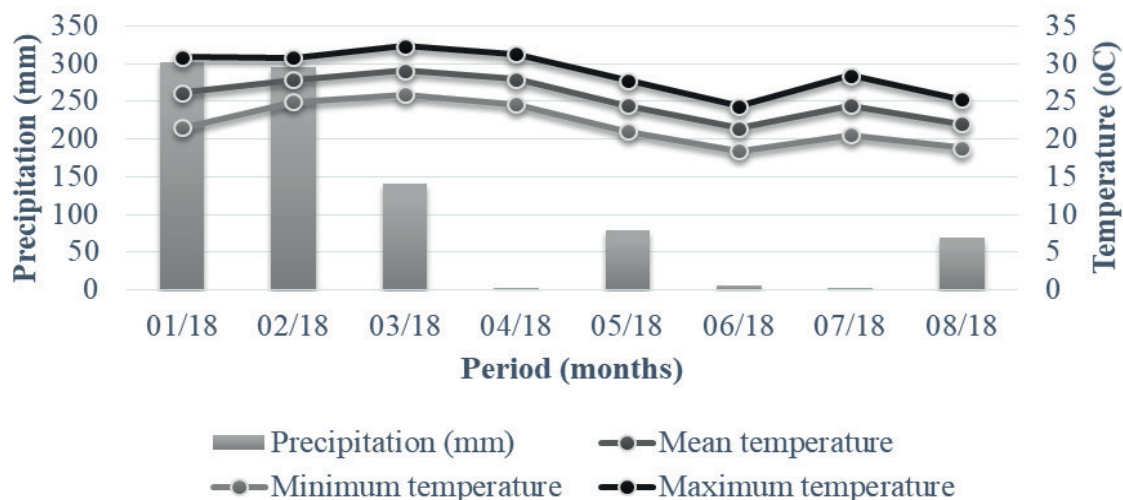


**Figure 1.** Mean data of precipitation and air temperature between January and August 2018, obtained from the weather station COAMO, Rod. MS 286 – KM 02, Aral Moreira, MS, Brazil.

**Table 1.** Components of the Sentinel-2A and Sentinel-2B imaging instruments.

Resolution (m)	Band	Band name	Wavelength (nm)
10	B2	Blue	490
	B3	Green	560
	B4	Red	665
20	B8	Near-infrared	842
	B5	Red edge	705

Nanometer (nm).

blue (band B2), green (band B3), red (band B4), and near-infrared (band B8) and 20 m for the red edge spectrum electromagnetic (band B5).

Atmospheric corrections were carried out in the images using the free software QGIS v. 2.18.24. The reflectance index of bands B2, B3, B4, B8, and B5 were corrected by transforming the top of atmosphere reflectance into surface reflectance (Pertille et al., 2018). The corrected images were transformed into the raster format with regular spacing of  $10 \times 10$  m, with each cell represented by a specific numerical value referring to the radiometric intensity of the pixel in nanometers (Molin et al., 2015). The VI equations were applied according to the recommendations of the respective authors.

Equation 1 (Rouse et al., 1974):

$$NDVI = (NIR - Red) / (NIR + Red)$$

where NDVI is the normalized difference vegetation index, NIR is the near-infrared wavelength, and Red is the red wavelength.

Equation 2 (Fitzgerald et al., 2006):

$$NDRE = (NIR - Red\ Edge) / (NIR + Red\ Edge)$$

where NDRE is the normalized difference red edge index, NIR is the near-infrared wavelength, and Red Edge the red edge wavelength.

Equation 3 (Gitelson & Merzlyak, 1998):

$$GNDVI = (NIR - Green) / (NIR + Green)$$

where GNDVI is the green normalized difference vegetation index, NIR is the near-infrared wavelength, and Green is the green wavelength.

Equation 4 (Fu-min et al., 2007):

$$GRNDVI = NIR - (Green + Red) / NIR + (Green + Red)$$

where GRNDVI is the green-red normalized difference vegetation index, NIR is the near-infrared wavelength, Green is the green wavelength, and Red is the red wavelength.

Equation 5 (Fu-min et al., 2007):

$$\text{PNDVI} = \text{NIR} - (\text{Green} + \text{Red} + \text{Blue}) / \text{NIR} + (\text{Green} + \text{Red} + \text{Blue})$$

where PNDVI is the pan normalized difference vegetation index with green, red, and blue, NIR is the near-infrared wavelength, Green is the green wavelength, Red is the red wavelength, and Blue is the blue wavelength.

The GRNDVI and PNDVI equations follow the principle of the same sequence exposed by Fu-min et al. (2007), but with the replacement of the red wavelength with the red edge. In this case, their nomenclatures were changed to GRENDVI and PRENDVI.

Equation 6 (adapted from Fu-min et al., 2007):

$$\text{GRENDVI} = \text{NIR} - (\text{Green} + \text{Red Edge}) / \text{NIR} + (\text{Green} + \text{Red Edge})$$

where GRENDVI is the green-red edge normalized difference vegetation index, NIR is the near-infrared wavelength, Green is the green wavelength, and Red Edge the red edge wavelength.

Equation 7 (adapted from Fu-min et al., 2007):

$$\text{PRENDVI} = \text{NIR} - (\text{Green} + \text{Red Edge} + \text{Blue}) / \text{NIR} + (\text{Green} + \text{Red Edge} + \text{Blue})$$

where PRENDVI is the pan normalized difference vegetation index with green, red edge, and blue, NIR is the near-infrared wavelength, Green is the green wavelength, Red Edge is the red edge wavelength, and Blue is the blue wavelength.

The grain yield data were collected every

second by a grain harvester with a satellite navigation system, panel, and onboard sensors. The collected point cloud was treated, and the final product consisted of georeferenced point data and respective yield. The data were georeferenced in the UTM (Universal Transverse Mercator) format and the yield was expressed in  $\text{kg ha}^{-1}$  (Acosta et al., 2018). The set of information was manipulated to eliminate discrepant data through the standard deviation (Barbosa & Maldonado, 2015). Subsequently, the point data were interpolated by the inverse distance weighted method, generating a file in raster format, with each pixel representing local georeferenced data on the yield obtained in the field. The area was divided into 1925 plots and each plot consisted of a  $10 \times 10$ -m pixel.

The yield and VI maps were classified into three intensities for the distinction between sample classes, which are high, medium, and low. Maps were generated representing regions with different estimates of corn yield based on each VI.

The grain yield and VI data were compared by correlation analysis and linear regression.

## Results and discussion

The mean values of VIs were discrepant although all images were obtained on the same date, allowing the differentiation between those with higher (GNDVI and NDVI) and lower values (PRENDVI and PNDVI) (Table 2).

**Table 2.** Descriptive statistics of vegetation indices and grain yield.

	<b>M</b>	<b>A</b>	<b>V</b>	<b>SD</b>	<b>SEM</b>	<b>CV</b>
PRENDVI	0.21	0.31	0.004	0.06	0.001	31.05
PNDVI	0.28	0.37	0.005	0.07	0.001	26.28
GRENDVI	0.32	0.29	0.004	0.06	0.001	19.00
GRNDVI	0.39	0.35	0.005	0.07	0.001	17.23
NDRE	0.51	0.26	0.003	0.05	0.001	10.40
NDVI	0.62	0.33	0.004	0.06	0.001	10.05
GNDVI	0.67	0.16	0.001	0.03	0.001	4.86
Yield	2917.32	4173.00	960302.515	979.95	22.335	33.59

Mean (M) VI in nanometer and yield in kg ha<sup>-1</sup>; amplitude (A); variance (V); standard deviation (SD); standard error of the mean (SEM); coefficient of variation (CV, %); pan normalized difference vegetation index with green, red edge, and blue (PRENDVI); pan normalized difference vegetation index with green, red, and blue (PNDVI); green-red edge normalized difference vegetation index (GRENDVI); green-red normalized difference vegetation index (GRNDVI); normalized difference red edge index (NDRE); normalized difference vegetation index (NDVI); green normalized difference vegetation index (GNDVI).

The lowest coefficients of variation were also observed for GNDVI, NDVI, and NDRE (Table 2), indicating a higher precision of the data and, therefore, a lower sampling error.

The box plot with the mean data of VIs (Figure 2) indicated that GNDVI and NDVI were the most sensitive to physiological changes in the crop canopy, with the lowest standard deviation of the mean. Despite this, the indices GNDVI and NDVI tended to a fast saturation, reaching their maximum value in a short period, which may compromise the distinction between sample classes, while the indices NDRE, GRNDVI, PNDVI, GRENDVI, and PRENDVI, which had a higher standard deviation of the mean, allowed for categorical distinction and demanded more time for saturation.

The replacement of the red wavelength with the red edge (NDRE, GRENDVI, and PRENDVI) in the VI equations provided better correlation results with grain yield (Table 3).

Kanke et al. (2016) observed that the VIs used with red edge tended to improve rice yield forecasting algorithm and have a higher degree of linear relationship with biomass, N absorption, and grain yield than indices based on the red wavelength. There are also reports of a better correlation with the leaf area index (Fu-min et al., 2007).

According to Vian et al. (2018), the production potential of the corn crop can be estimated using NDVI. However, the comparison of VIs in Table 4 showed that NDVI is one of the indices with the lowest correlation with yield.

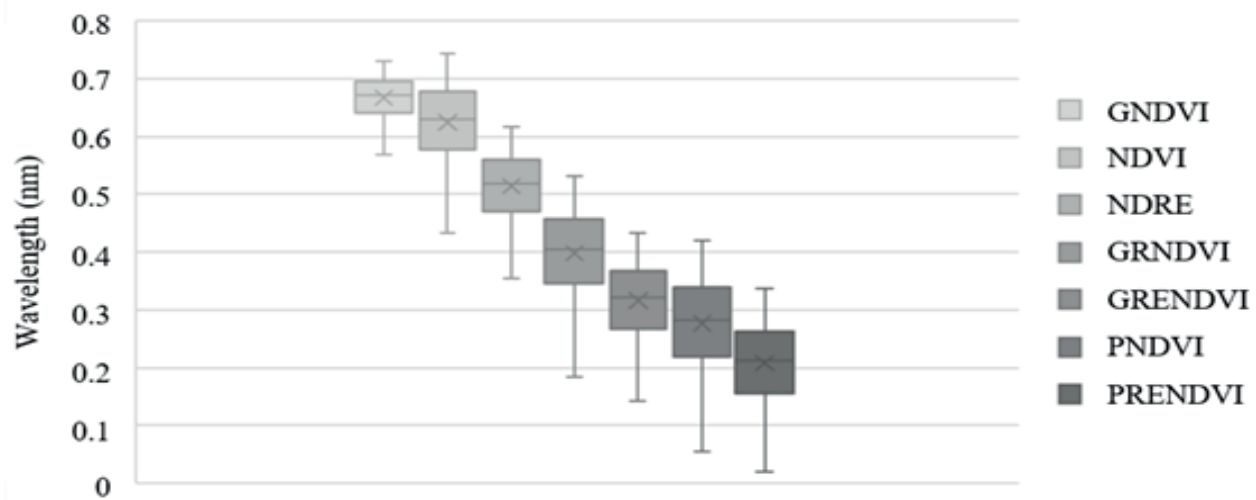


**Figure 2.** Box plot with mean vegetation index data; nanometers (nm); pan normalized difference vegetation index with green, red edge, and blue (PRENDVI); pan normalized difference vegetation index with green, red, and blue (PNDVI); green-red edge normalized difference vegetation index (GRENDVI); green-red normalized difference vegetation index (GRNDVI); normalized difference red edge index (NDRE); normalized difference vegetation index (NDVI); green normalized difference vegetation index (GNDVI).

**Table 3.** Correlation matrix between vegetation indices and grain yield.

VI	YIELD	PRENDVI	PNDVI	GRENDVI	GRNDVI	NDRE	NDVI
PRENDVI	0.85**	–	–	–	–	–	–
PNDVI	0.84**	0.99**	–	–	–	–	–
GRENDVI	0.85**	0.99**	0.99**	–	–	–	–
GRNDVI	0.84**	0.99*	0.99*	0.99**	–	–	–
NDRE	0.85**	0.99**	0.99**	0.99**	0.99**	–	–
NDVI	0.83**	0.99**	0.99**	0.99**	0.99**	0.99**	–
GNDVI	0.84**	0.99**	0.98**	0.99**	0.99**	0.98**	0.99**

Pearson's correlation coefficient \*\* ( $p < 0.001$ ) using the T-test; grain yield (YIELD); pan normalized difference vegetation index with green, red edge, and blue (PRENDVI); pan normalized difference vegetation index with green, red, and blue (PNDVI); green-red edge normalized difference vegetation index (GRENDVI); green-red normalized difference vegetation index (GRNDVI); normalized difference red edge index (NDRE); normalized difference vegetation index (NDVI); green normalized difference vegetation index (GNDVI).

Bagheri et al. (2013) studied VIs in corn and found correlations through a polynomial equation with nitrogen doses, with NDVI also presenting

the lowest correlation. This fact, associated with the data inherent to this experiment, indicates that NDVI is not one of the best estimators for

**Table 4.** Mean grain yield obtained by mean indices.

Variable					
Dep. Y	Ind. X	Equation	Yield	R <sup>2</sup>	F
Yield	PRENDVI	$Y=12936.75X+234.03$	2950.74	0.72	5013.21**
	PNDVI	$Y=11325.65X-215.31$	2995.69	0.71	4613.73**
	GRENDVI	$Y=13860.66X-1464.60$	2970.81	0.72	4990.26**
	GRNDVI	$Y=11935.14X-1840.99$	2813.71	0.70	4494.72**
	NDRE	$Y=15507.86X-5054.74$	2854.27	0.71	4841.73**
	NDVI	$Y=12925.97X-5151.08$	2863.02	0.68	4176.52**
	GNDVI	$Y=25442.90X-14053.93$	2992.81	0.71	4674.04**

Dependent variable (Dep. Y); independent variable (Ind. X); mean yield in kg ha<sup>-1</sup> (Yield); coefficient of determination (R<sup>2</sup>); analysis of variance for linear regression (F); \*\* (p<0.001); pan normalized difference vegetation index with green, red edge, and blue (PRENDVI); pan normalized difference vegetation index with green, red, and blue (PNDVI); green-red edge normalized difference vegetation index (GRENDVI); green-red normalized difference vegetation index (GRNDVI); normalized difference red edge index (NDRE); normalized difference vegetation index (NDVI); green normalized difference vegetation index (GNDVI).

corn yield in the field.

The grain yield map and VIs (Figure 3) showed that PRENDVI, GRENDVI, PNDVI, and GRNDVI are indices that take longer to saturate, an effect observed in maps due to the presence of wavelengths from 0.02 to 0.5 nm, which are low values compared to the indices NDRE, NDVI, and GNDVI, which showed wavelengths from 0.3 to 0.7 nm. The same observations can be found in the linear regression graphs between grain yield and VIs (Figure 4). Vian et al. (2018) observed that different areas and/or regions of corn grain yield can be identified through VIs.

Grain yield has high spatial variability

(Figure 3), which can be correlated with a different crop, such as the distribution and final population of plants, and the spatial variability of soil attributes. According to Vian et al. (2016), the highest corn grain yields depend on the final population and the uniform spatial distribution of plants, with the final number of ears per area being the component that most contributes to grain yield. Bernardi et al. (2017) also found a correlation between VIs and soil attributes in the corn crop, being an indicator of variations used for defining management zones and map generation. Thus, Figure 3 allowed identifying regions with different corn grain yields and VI intensities. The



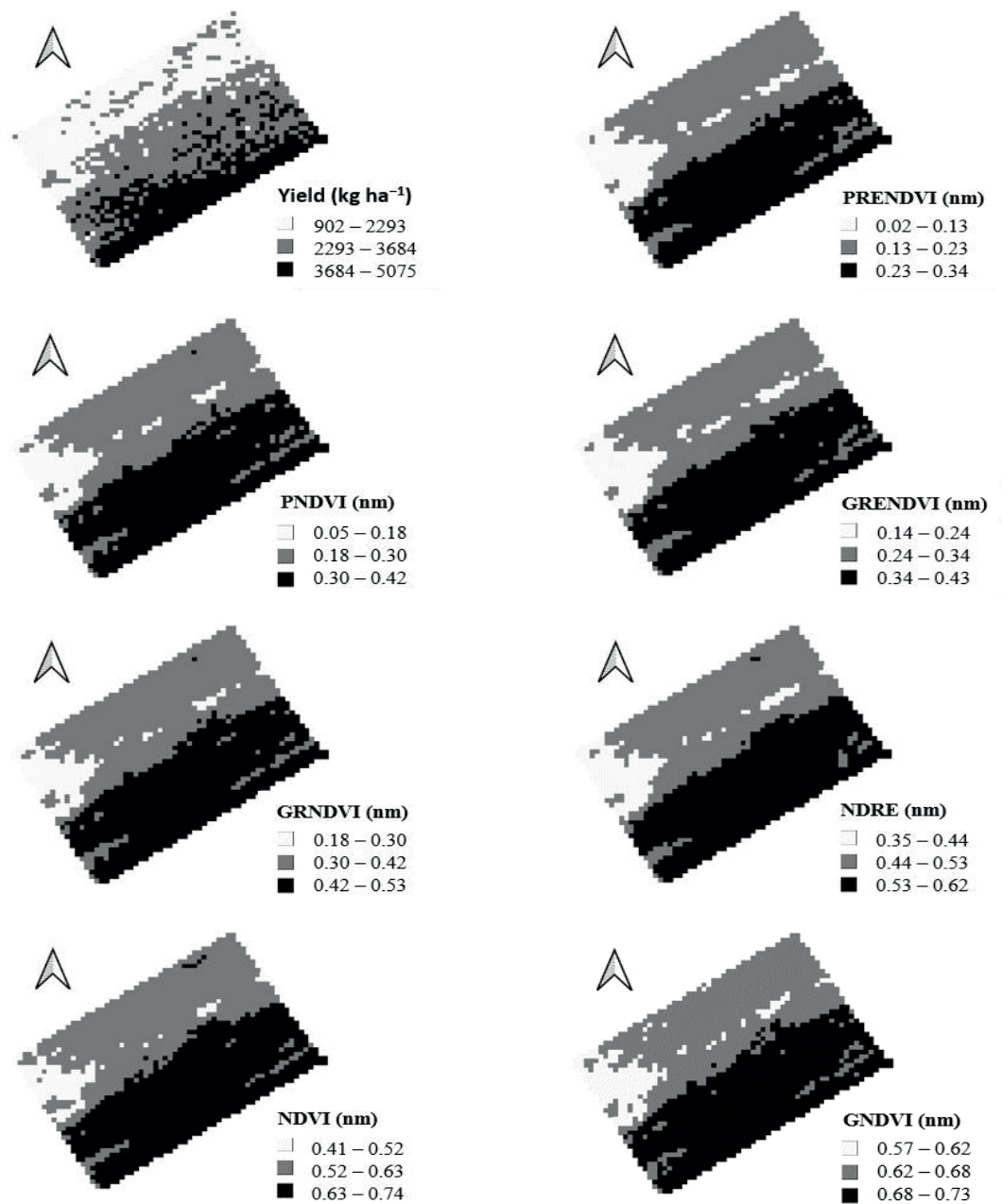


**Figure 3.** Grain yield maps sampled and estimated from vegetation indices. Grain yield (Yield); nanometers (nm); pan normalized difference vegetation index with green, red edge, and blue (PRENDVI); pan normalized difference vegetation index with green, red, and blue (PNDVI); green-red edge normalized difference vegetation index (GRENDVI); green-red normalized difference vegetation index (GRNDVI); normalized difference red edge index (NDRE); normalized difference vegetation index (NDVI); green normalized difference vegetation index (GNDVI).

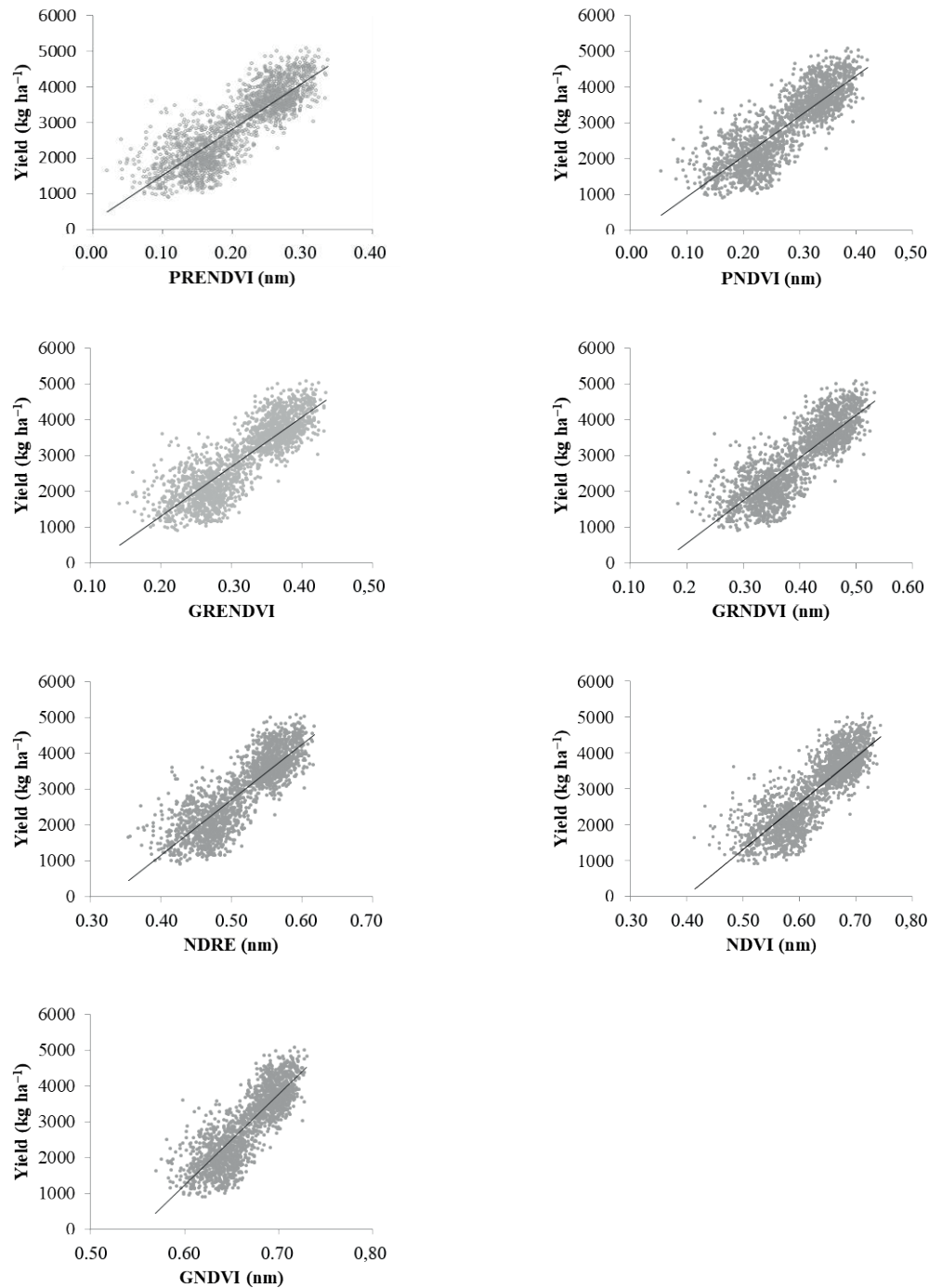


**Figure 4.** Linear regression analysis between grain yield and VIs. Pan normalized difference vegetation index with green, red edge, and blue (PRENDVI); pan normalized difference vegetation index with green, red, and blue (PNDVI); green-red edge normalized difference vegetation index (GRENDVI); green-red normalized difference vegetation index (GRNDVI); normalized difference red edge index (NDRE); normalized difference vegetation index (NDVI); green normalized difference vegetation index (GNDVI).

yield map and VIs (Figure 3) were categorized into three sample classes, namely, low, medium, and high.

The mean values, represented by the coefficient of determination ( $R^2$ ) and grain yield, were around 70%. Only NDVI presented values below 70% (Table 4). Vian et al. (2018) evaluated the estimate of corn grain yield using VIs from the phenological stages V3 (third pair of leaves) to VT (full tasseling) and observed coefficients of determination ( $R^2$ ) between 0.63 and 0.83, respectively, with increasing correlations as the plant grows. Higher VI values indicate higher grain yield.

The results of the linear regressions indicated that all VIs can be used to estimate the mean corn grain yield in the field (Table 4). However, some VIs tend to a fast saturation in a short period, such as GNDVI and NDVI, making it difficult to distinguish between sample classes. Therefore, the best indices for estimating the mean corn grain yield in the field were PRENDVI and GRENDVI.

### Conclusions

The indices GNDVI and NDVI showed a fast saturation, reaching maximum values that compromised the distinction between yield classes.

The VIs in which the red edge was considered had better estimates and higher correlations with the corn grain yield in the field.

The recommended VIs for estimating

corn grain yield in the field are PRENDVI and GRENDVI.

### Acknowledgments

To Capes for granting the doctoral scholarship to the first author.

### References

- ACOSTA, J. J. B.; CABRERA, M.G.; IBRAS, R. F.; GONZÁLEZ, J.G.; CHAMORRO, A. M.; ECOBAR, J. Variabilidade espacial da produtividade, perdas na colheita e lucratividade da cultura de soja. **Revista Agrogeoambiental**, v. 10, n. 1, p. 27-46, 2018. DOI: [10.18406/2316-1817v10n120181050](https://doi.org/10.18406/2316-1817v10n120181050).
- BAGHERI, N.A.; AHMADI, H.; ALAVIPANAH, S. K.; OMID, M. Multispectral remote sensing for site specific nitrogen fertilizer management. **Pesquisa Agropecuária Brasileira**, v. 48, n.10, p. 1394-1401, 2013. DOI: [10.1590/S0100-204X2013001000011](https://doi.org/10.1590/S0100-204X2013001000011).
- BARBOSA, J. C.; MALDONADO, J. W. **Experimentação Agronômica e AgroEstat**. Jaboticabal, 2015. 396 p.
- BERTOLIN, N. O.; ROBERTO, F.; LUAN, P. V.; EVERARDO, C. M. Predição da produtividade de milho irrigado com auxílio de imagens de satélite. **Revista Brasileira de Agricultura Irrigada**, v. 11, n. 4, p. 1627-1638, 2017. DOI: [10.18512/rbms2021v20e1195](https://doi.org/10.18512/rbms2021v20e1195)

[10.7127/rbai.v11n400567](https://doi.org/10.7127/rbai.v11n400567).

BERNARDI, A. C. C.; GREGO, C. R.; ANDRADE, R. C.; RABELLO, L. M.; INAMASU, RY. Spatial variability of vegetation index and soil properties in an integrated crop-livestock system. **Revista Brasileira de Engenharia Agrícola e Ambiental**, v. 21, p. 513-518, 2017. DOI: [10.1590/1807-1929/agriambi.v21n8p513-518](https://doi.org/10.1590/1807-1929/agriambi.v21n8p513-518).

CUI, Z.; REKES, K. P. Potential of red edge spectral bands in future landsat satellites on agroecosystem canopy green leaf area index retrieval. **Remote Sensing**, v.10, n. 9, p. 1-14, 2018. DOI: [10.3390/rs10091458](https://doi.org/10.3390/rs10091458).

CONTINI, E.; MOTA, M. M.; MARRA, R.; BORGHI, E.; MIRANDA, R. A. de; SILVA, A. F.; SILVA, D. D.; MACHADO, J. R. A.; COTA, L. V.; COSTA, R. V.; MENDES, S. M. Serie desafios do grande negócio brasileiro. **Milho: caracterizações e desafios tecnológicos**. Brasília, DF: Embrapa; Sete Lagoas: Embrapa Milho e Sorgo, 2019. 45 p.

EARTHEXPLORER. Available in: <<https://earthexplorer.usgs.gov>>. Access in: 13 May 2018.

FITZGERALD, G.J.; RODRIGUEZ, D.; CHRISTENSEN, L. K.; BELFORD, R.; SADRAS, V. O.; CLARKE, T. R. Spectral and thermal sensing for nitrogen and water status in rainfed and irrigated wheat environments. **Precision Agriculture**, v. 7, n. 4, p. 233–248, 2006. DOI: [10.1007/s11119-006-9011-z](https://doi.org/10.1007/s11119-006-9011-z).

FU-MIN, W.; JING-FENG, H.; YAN-LIN, T.; XIU-ZHEN, W. New Vegetation Index and Its Application in Estimating Leaf Area Index of Rice. **Rice Science**, v. 14, n. 3, p. 195-203, 2007. DOI: [10.1016/S1672-6308\(07\)60027-4](https://doi.org/10.1016/S1672-6308(07)60027-4).

GITELSON, A. A.; MERZLYAK, M. Remote Sensing of Chlorophyll Concentration in Higher Plant Leaves. **Advances in Space Research**, v. 22, n. 5, p.689-692, 1998. DOI: [10.1016/S0273-1177\(97\)01133-2](https://doi.org/10.1016/S0273-1177(97)01133-2).

KÖPPEN, W. E GEIGER, R. Handbuch der Klimatologie. **Gebrüder Bornträger**, p. 1-44, 1936.

KANKE, Y, TUBAÑA, B, DALEN, M E HARRELL, D. Evaluation of red and red-edge reflectance-based vegetation indices for rice biomass and grain yield prediction models in paddy fields. **Precision Agriculture** v. 17, n.5, p. 507-530, 2016. DOI: [10.1007/s11119-016-9433-1](https://doi.org/10.1007/s11119-016-9433-1).

MOLIN, J. P.; RIOS, A. M.; COLAÇO, A. M. **Agricultura de precisão**. Piracicaba: Oficina de Textos, 2015. 233 p. Disponível em: <https://www.bibliotecaagptea.org.br/agricultura/precisao/livros/AGRICULTURA%20DE%20PRECISAO%20-%20OFICINA%20DE%20TEXTOS.pdf>. Acesso em: 21 maio 2018.

NGIE, A.; AHAMED, F. Estimation of Maize grain yield using multispectral satellite data sets

- (SPOT 5) and the random forest algorithm. South African Journal of Geomatics, v. 7, n. 1, p. 11-30, 2018. DOI: [10.4314/sajg.v7i1.2](https://doi.org/10.4314/sajg.v7i1.2).
- PERTILLE1, CT, SILVA, GO, SOUZA, CF E NICOLETTI, MF. Estudo da eficiência de classificações supervisionadas aplicadas em imagem de média resolução espacial. BIOFIX Scientific Journal, v. 3, n. 2, p. 289-296, 2018. DOI: [10.5380/biofix.v3i2.60477](https://doi.org/10.5380/biofix.v3i2.60477).
- ROSA, A. P. S. A.; EMYGDIO, B.M.; BISPO, N. B. **Indicações Técnicas para o Cultivo de Milho e de Sorgo no Rio Grande do Sul Safras 2017/2018 e 2018/2019**. Brasília, Embrapa Clima Temperado, 2017. 209 p.
- ROUSE, JW. HAAS, RH. WELL JÁ E DEERING, DW. Monitoring vegetation systems in the great plains with ERTS. **Goddard Space Flight Center**, v.1, p. 309-317, 1973.
- SANTOS, H. G.; JACOMINE, P. K. T.; ANJOS, L. H. C.; OLIVEIRA, V. A.; LUMBRERAS, J.F.; COELHO, M. R.; ALMEIDA, J. A; ARAÚJO, J. C.; OLIVEIRA, J.B.; CUNHA, T. J. F. Sistema Brasileiro de Classificação de Solos. 2018. Disponível em: <<http://ainfo.cnptia.embrapa.br/digital/bitstream/item/181678/1/SiBCS-2018-ISBN-9788570358219-english.epub>>. Acessado em 21 maio 2018.
- VIAN, A. L.; SANTI, A. L.; AMADO, T. J. C; CHERUBIN, M. R.; SIMON, D. H.; DAMIAN J. M.; BREDEMEIER, C. Variabilidade espacial da produtividade de milho irrigado e sua correlação com variáveis explicativas de planta. *Ciência Rural*, v. 46, n. 3, p. 464-471, 2016. DOI: [10.1590/0103-8478cr20150539](https://doi.org/10.1590/0103-8478cr20150539).
- VIAN, A. L.; BREDEMEIER, C.; SILVA, P. R. F.; SANTI, A. L.; GIORDANO, C. P. S.; SANTOS, F. L. Limites críticos de NDVI para estimativa do potencial produtivo do milho. *Revista Brasileira de Milho e Sorgo*, v. 17, n. 1, p. 91-100, 2018. DOI: [10.18512/1980-6477/rbms.v17n1p91-100](https://doi.org/10.18512/1980-6477/rbms.v17n1p91-100).
- YAMAMOTO, K. Y.; LANDIM, P. M. B. **Geoestatística conceitos e aplicação**. Jaboticabal: Oficina de Textos, 2013. 215 p.